

AN ENHANCED ESTIMATION OF COLLAPSE FRAGILITY OF RC BUILDINGS

*M. Ebrahimi Koopae¹, R. P. Dhakal¹, Gregory MacRae¹

¹ *Department of Civil and Natural Resources Engineering, University of Canterbury, Christchurch, New Zealand*

ABSTRACT

This paper investigates several aspects of collapse assessment of RC buildings through a case study building designed based on New Zealand standards. A fiber-element based analysis is first introduced to simulate structural collapse which captures loss of vertical load carrying capacity of structural components. The fiber model uses generic path-dependent cyclic stress-strain relationships of concrete and reinforcing steels, which enable the analysis to capture cyclic strength deterioration and consequent failure due to low cycle fatigue and buckling of reinforcing bars. At the next stage, instead of conducting conventional incremental dynamic analysis (IDA) to generate collapse fragility curve, response history analyses (RHAs) are performed at discrete hazard levels. Collapse probabilities at various hazard levels are then fitted to a lognormal distribution to construct the collapse fragility curve. In order to investigate the variation of collapse fragility curve using different ground motion (GM) selection approaches, two alternatives of uniform hazard spectrum (UHS), conditional mean spectrum (CMS), and generalised conditional mean spectrum (GCIM) are used to select GMs at each hazard level. To match selected GMs to a target spectrum, where required, a more convincing period range dependent on the structural characteristics is introduced. A new source of uncertainty in estimation of collapse fragility of buildings is introduced to account for the variability due to different GM selection methods available.

Keywords: Fiber-element modelling, collapse fragility curve, ground motion selection

1 INTRODUCTION

Current building codes are generally silent on the ways to quantify life safety which is directly related to the collapse probability of structural systems. The lack of explicit methods to quantify collapse in current codes is an impediment to application of performance-based seismic design guidelines, understanding the necessity and significance of modern code requirements, as well as development and adoption of innovative and efficient seismic systems and components.

Advancements of the past two decades in structural models and analysis have made it possible to simulate some of the collapse modes of buildings under earthquake ground

motions (GMs). Major improvements in structural models for seismic collapse quantification of buildings have been made since the work of Ibarra, Medina and Krawinkler (2005) who developed an enhanced hysteretic model by incorporating various kinds of stiffness and strength degradation combined with $P-\Delta$ effects to capture sidesway mode of collapse. Since the introduction of this structural model, majority of research in structural modelling for collapse simulation have been concentrated on the development and improvement of nonlinear lumped plasticity models. These models capture sidesway collapse mode of buildings when the lateral strength and stiffness become insufficient to resist destabilizing $P-\Delta$ effects; thereby leading to large interstorey drifts (e.g Haselton 2006, Zareian and Krawinkler 2007, Liel 2008, Lignos and Krawinkler 2012).

Structural collapse analysis based on lumped plasticity nonlinear modelling inherently suffers from several drawbacks. Most significant among these drawbacks is its inability to capture the loss of vertical load carrying capacity of one or more components in the structure, such as loss in axial capacity of columns. During cyclic excitations, loss in the axial capacity of vertical elements can occur prior to occurrence of large inter-storey drifts when the building may still resist destabilizing $P-\Delta$ effects. Moreover, lumped plasticity models have to be calibrated for individual sections based on experimental results or predetermined generic quantities have to be used (e.g. Haselton et al. 2008) which may result in further errors within the assessment procedure. Another limitation of lumped plasticity model is its inability to capture the variation of moment capacity of the same cross-section due to the inevitable variation of axial force during lateral cyclic excitation.

Incremental Dynamic Analysis (IDA) (Vamvatsikos & Cornell 2002) has been commonly used in current methods for probabilistic collapse assessment of buildings using one suite of GMs scaled to include a wide range of responses from elastic to collapse. Individual GMs in this method are assumed to represent various hazard intensities merely by scaling the GM to match the intensity measure corresponding to the required hazard level. However, since large scale factors are often required for the selected GMs to cause collapse, selected records do not realistically represent the severe hazard intensity in terms of duration, energy content and frequency content of GMs.

This paper presents a discussion on various aspects of seismic collapse risk assessment of RC buildings by (i) application of a fiber-element based analysis to simulate structural collapse including the loss in vertical load carrying capacity of structural elements; (ii) conducting RHAs at discrete hazard levels using different sets of GMs representative of the hazard level being considered to obtain the collapse fragility curve; and (iii) comparison of different GM selection approaches in terms of their collapse prediction efficiency at various hazard intensities. The paper also explains the vertical collapse mechanism of RC buildings and introduces a fiber element-based structural model which can capture this mechanism. A methodology is then implemented for collapse assessment of a case study RC building by conducting RHAs at discrete hazard levels using several GM selection methods. Eventually, the uncertainty arising from GM selection

is quantified which can be used in collapse risk assessment using a single GM selection method.

2 FIBER-ELEMENT BASED MODELLING OF STRUCTURAL COLLAPSE

2.1 Collapse mechanism of RC buildings

Collapse of a building occurs due to local and/or global failure of sufficient number of structural components to cause instability. At the component/element level, failure occurs due to failure of a critical section, which is because of the materials reaching the ultimate strain.

In an RC element subjected to monotonically increasing flexural action, cover concrete is first spalled at the critical section once the strain in the unconfined concrete reaches its crushing strain. Following the loss of cover concrete, the section resistance will rely increasingly on the confined core concrete in addition to the longitudinal reinforcing bars. If the compression bars are not well restrained against buckling, or if adequate transverse reinforcement is not provided, the critical section may fail in shear, or buckling of longitudinal bars may occur before the core concrete reaches its crushing strain. In contrast, in a well confined section, confinement of core concrete allows longitudinal tension bars to enter the strain hardening region. In such sections, failure of the section eventually occurs due to failure of the core concrete. If the section is over-reinforced, this failure occurs before yielding of longitudinal bars, whereas in under-reinforced sections (as this is the case in code-conforming sections), yielding of longitudinal bars takes place before crushing of the core concrete. In cyclic loading of a well confined section, in addition to the failure modes induced by monotonic loading, failure may also occur due to strength deterioration of the cracked concrete and longitudinal bars which can be caused by buckling of compression bars as well as fatigue of steel bars before the core concrete reaches to crushing strain.

2.2 Adopted fiber models for concrete and steel to simulate collapse

This section is devoted to explain the fiber models which are adopted in this paper to simulate structural collapse mechanism as discussed in the previous section. In order to simulate collapse of RC buildings, PEER's open source structural analysis and simulation tool OpenSees (2012) is utilized. In OpenSees, several material properties have been implemented which enable simulation of structural collapse. The adopted concrete and steel models are discussed in the following sections.

2.2.1 Confined and unconfined concrete

Popovics (1973) concrete model is used for modelling of confined and unconfined concrete. Fig. 1a and 1c illustrate respectively the typical monotonic and cyclic stress-strain history of the concrete fibers used in this study. This model requires specification of seven parameters to control monotonic behaviour of both confined and unconfined concrete: concrete compressive strength in 28 days f_c , concrete strain at maximum

strength ε_c , concrete strain at crushing strength ε_{cu} , initial stiffness E_c , maximum tensile strength of concrete f_{ct} , ultimate tensile strain of concrete ε_t , and an exponential curve parameter to define the residual stress β (optional).

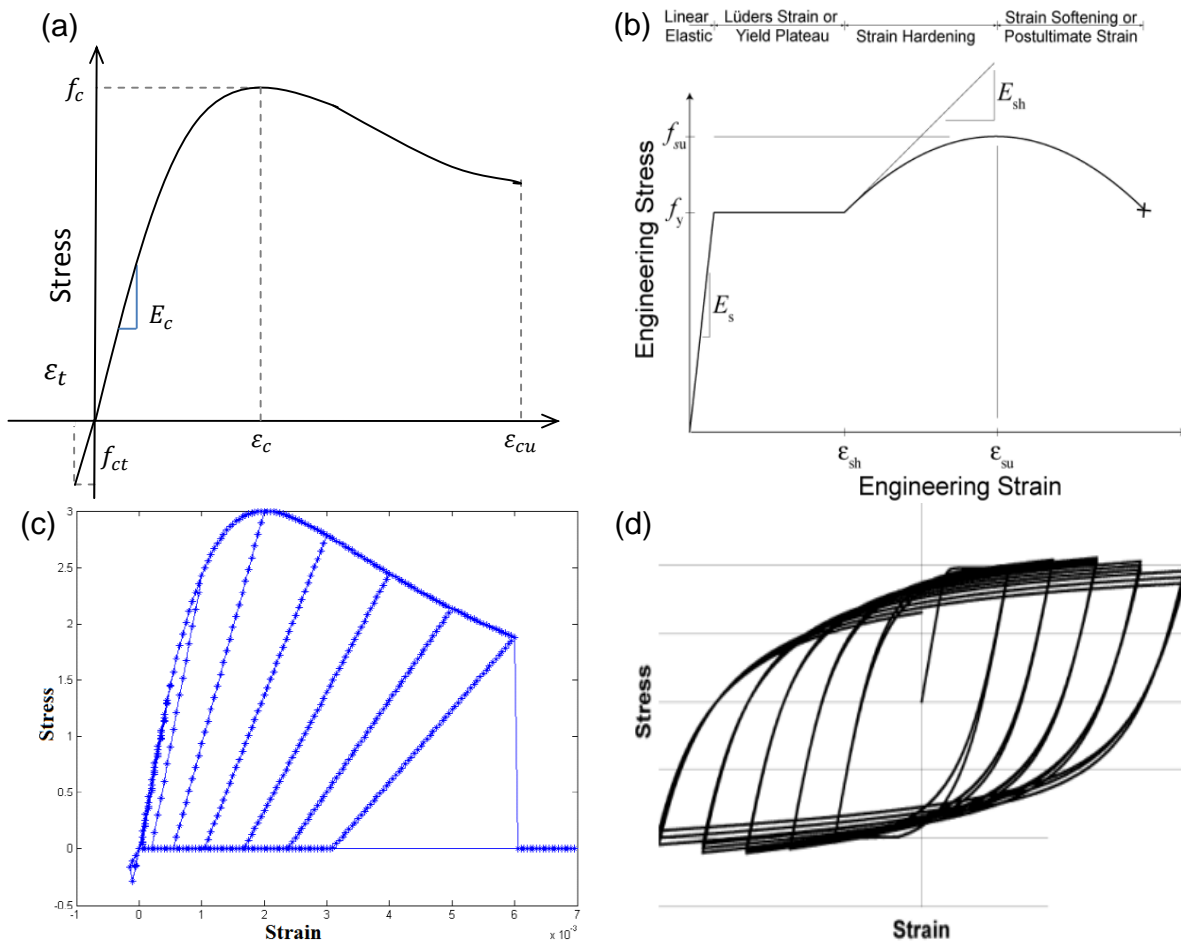


Fig. 1 Material models used in the study (a) Monotonic tension-compression envelope of Popovics model (b) Stress-strain envelope of the steel model (c) Cyclic behaviour of the concrete model (d) Cyclic behaviour of reinforcing steel model (figures adopted from the OpenSees (2012) website)

Parameters of the model can be obtained by a simple uniaxial experimental test. Alternatively, for practical purposes, compressive strength for unconfined concrete in 28 days can be obtained from the design documents of the structure. Other parameters can be estimated from the known f_c . Mander et al. (1988) have proposed a widely accepted theoretical stress-strain model for confined concrete, depending on the confinement configuration, which can be used to quantify the maximum stress and strain of confined

concrete. Approximate equations have been suggested in building codes for initial stiffness of concrete. If $E_c = 4734\sqrt{f_c}$ (in MPa) is used to estimate initial stiffness, then Popovics envelope model will be identical to the model proposed by Mander et al. (1988).

For collapse prediction, concrete strain at crushing is the most important parameter. Collapse capacity is directly dependent on this value, which is controlled by the confinement configuration of critical sections. Theoretical values of strain at the crushing point have been proposed in literature depending on the number, size, and spacing of transverse bars in the section (e.g. Karthik and Mander 2011). Based on the expressions proposed in literature to calculate the ultimate strain of confined concrete, common ductile detailing gives approximately an ultimate strain of $\varepsilon_{cu} = 0.03$ which will be used in this study for crushing strain of confined concrete.

2.2.2 Reinforcement steel model

In order to simulate the behaviour steel bars in RC sections, a generic model proposed by Kunnath et al. (2009), which accounts for the strength degradation due to fatigue in cyclic loading as well as buckling of reinforcing bars in compression, is utilized. Fig. 1b and 1d illustrate respectively a typical monotonic and cyclic stress-strain relationship of the reinforcing steel model. The envelope curve is based on the Chang and Mander (1994) uniaxial steel model. The degrading behaviour of RC section is influenced by buckling of longitudinal steel bars in compression, which is incorporated based on the model proposed by Dhakal and Maekawa (2002a, 2002b). Fatigue parameters are based on the Coffin-Manson equation for plastic strain amplitude. The softening region (strain beyond the ultimate stress point) shown in Fig. 1b is a localization effect due to necking and is a function of the gage length used during measurement. In this simulation, it is assumed that there is no softening in natural stress space. Because the simulation always converts back to engineering stress space, some softening will still be observed in the tension response due to the reduction in cross section area resulting from necking; however this will be much smaller than that shown in the original backbone curve proposed by Chang and Mander (1994).

Due to the nature of the steel model used herein, steel reinforcement failure may occur due to buckling of compression bars or fatigue of longitudinal bars after several cycles of loading, but pure tensile fracture (i.e. $\varepsilon_{su} \sim 0.1-0.2$) is not captured because the maximum steel stress is maintained beyond the peak strain. As will be shown in later sections, this does not influence the collapse simulations because concrete fibers crush and reach zero stress prior to the steel bars reaching their peak strain; thereby resulting in failure of the section. A peak strain of $\varepsilon_{su} = 0.1$ will be used in this paper as a conservative estimate for the steel bars used in New Zealand construction industry.

3 METHODOLOGY FOR GENERATING COLLAPSE FRAGILITY CURVE

The conventional approach for collapse assessment of buildings is to conduct IDA by performing a series of nonlinear RHAs in which the scale factors of a single set of selected

GMs are gradually increased until the last point at which the solution converges. The cumulative distribution function, assuming a lognormal distribution, of GM intensity measure (IM) values corresponding to structural collapse is defined as the 'collapse fragility curve' (Zareian and Krawinkler 2007). The collapse fragility curve shows the probability of collapse of a building at different intensity levels of a given ground motion IM . The conventional IDA approach of scaling a single suite of GMs to a wide range of intensities corresponding to different hazard levels has been a source of criticism as it cannot realistically represent various hazard intensities.

In response to the insufficiencies of IDA, in this paper, an alternative method for collapse assessment of buildings is adopted by selecting GMs and conducting RHAs at limited discrete hazard levels from low hazard intensities to rare, severe events. At different hazard levels, the collapse probability (i.e. $P(C|IM)$) is calculated as the number of GMs causing collapse divided by the total number of GMs used in the RHA at the hazard level. Then, the cumulative distribution function, assuming a lognormal distribution, of collapse probability values at discrete hazard levels defines the collapse fragility curve. The statistical procedure to fit the data points to a lognormal distribution will be explained in later sections. The lognormal distribution is used as previous studies have concluded, based on goodness-of-fit tests, that collapse intensities can be assumed to be lognormally distributed (Ibarra & Krawinkler 2005; Bradley & Dhakal 2008; Ghafory-Ashtiany et al. 2011). The RHAs should include low hazard levels, where the collapse probability is zero, and have to be continued until the level where most of the GMs cause collapse. Accuracy of the method depends on the accuracy of structural model, proper selection and scaling of GMs at various hazard levels, as well as the number of hazard levels considered to perform RHAs. Selection of more hazard levels, and computing the collapse probabilities at each level, provides further data points for statistical analysis to fit discrete collapse probabilities to a distribution. Furthermore, it is important to have sufficient data points scattered within a wide range of probabilities to get the best fit curve. However, recent studies have shown that intensities less than the structure's median collapse intensity typically have the largest contribution to the annual rate of building collapse (Bradley & Dhakal 2008; Eads et al. 2012). Therefore, the information on the first half of the collapse fragility curve, i.e. collapse probabilities up to 50%, are typically sufficient to construct the collapse fragility curve.

4 DETAILS OF THE CASE STUDY BUILDING

The described method is applied to the ten-storey New Zealand Red Book building (Bull and Brunsdon 1998), which acts as a design example of the 1995 New Zealand Concrete Standard. Fig. 2 shows the plan and elevation views of the building layout. The primary lateral load carrying system consists of four one-way perimeter moment resisting frames which are three bays long. Vertical loads are transferred primarily through interior columns with gravity beams supporting one-way floor units. Further details of the structural properties and design details can be found in Bull and Brunsdon (1998).

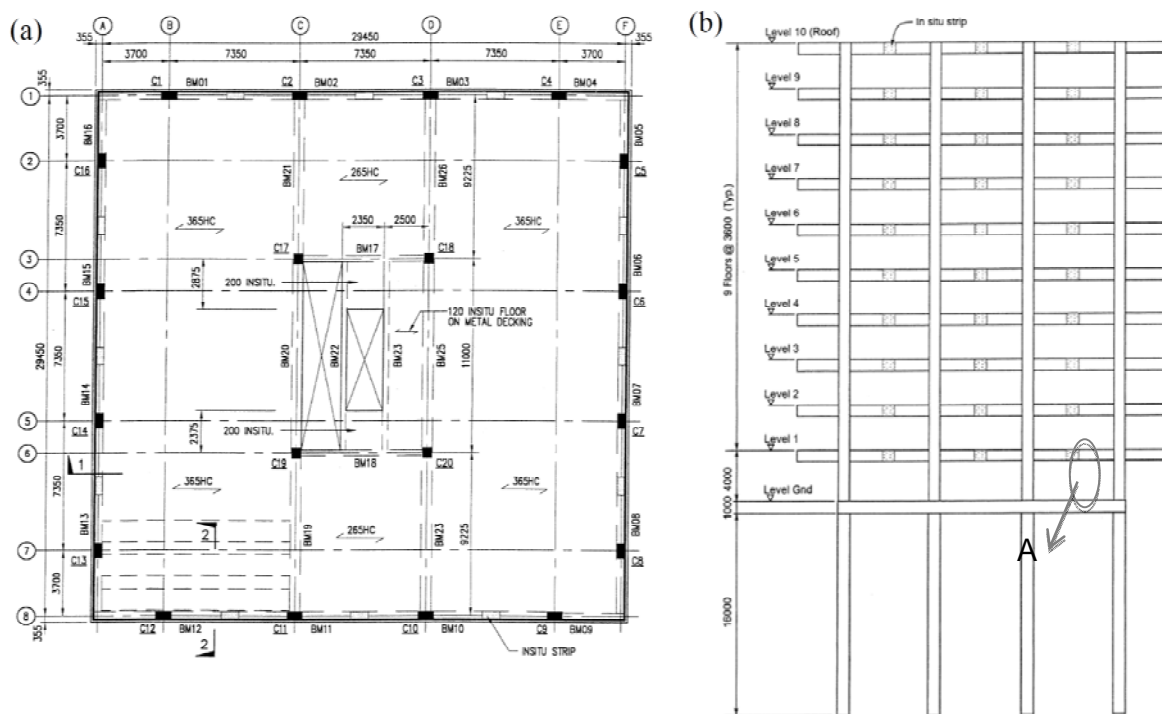


Fig. 2 Plan and elevation view of the New Zealand Red Book building used as the case study

The building is assumed to be located in Christchurch, New Zealand (longitude 172.6, latitude -43.53) and has been designed for soil class C based on the NZ loadings standard (NZS1170.5 2004) site classification.

A fiber-based 2D model of the perimeter frame is developed in OpenSees (2012) using the material models explained in the previous sections. A fiber-based section analysis was performed to identify the cracked stiffness of structural sections. Based on this analysis stiffness reduction factors of 0.63 and 0.42 were used for beam and column sections respectively to account for cracking. Using the cracked stiffness of structural components the period of the first mode amounts to $T_1 = 1.54s \cong 1.50s$.

4 GROUND MOTION SELECTION AT INDIVIDUAL HAZARD LEVELS

To evaluate the influence of the GM selection methods on the prediction of collapse fragility curve of RC buildings, in this paper, UHS, CMS (Baker and Cornell 2005, Baker 2011), and GCIM (Bradley 2010, 2012) based ground motion selection methods are used to select the earthquake records at discrete hazard levels. Collapse probabilities of the case study frame obtained by using the different sets of GMs are then compared. The procedure of GM selection based on various methods is explained in the following sections.

4.1 Selection of ground motions based on UHS

A probabilistic seismic hazard analysis is conducted to obtain the UHS at the site which is then used as the target spectrum to select GMs. According to the NZ code soil classification, shear wave velocity of the soil is selected to be $V_s(30) = 300$ m/sec. Figure 3 illustrates the resulting UHS for a range of periods for 2500-year return period superimposed with CMS conditioned on $S_a(T_1 = 1.5s)$, and NZS1170 (2004) spectrum which is similar to the design spectrum used in designing the building. As an alternative to the spectrum obtained by PSHA, NZS1170 design spectrum is also used as the target spectrum to select GMs. Therefore, two alternatives of UHS are examined in this paper. Throughout the paper where the UHS is obtained by conducting a PSHA, the method is termed as “PSHA” for brevity. Likewise, when the UHS is obtained by the NZS1170 spectra as the target the method is termed “NZS1170”, although the ground motion selection approach is not similar to the method stipulated in NZS1170 (2004).

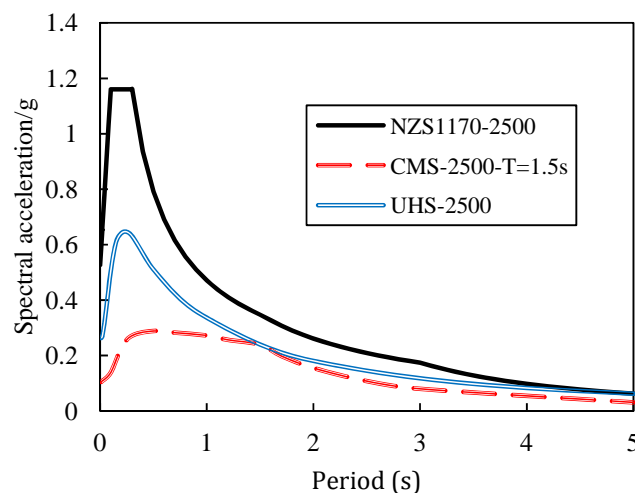


Fig. 3 Comparison of the CMS conditioned on $S_a(T_1 = 1.5s)$, UHS by PSHA and NZS1170 design spectrum for 2500 years return period

Figure 3 indicates that the two forms of UHS, i.e. obtained by NZS 1170 and via PSHA, agree in terms of spectral shape, but the code spectrum predicts significantly greater spectral accelerations compared to the values obtained by PSHA. The difference between these curves comes mainly from; (i) the code spectra are generally generated conservatively for design purposes; and (ii) selection of the shear wave velocity greatly affects the UHS obtained by a PSHA. For soil class C, the code stipulates a range of shear wave velocity rather than a single value. Using lower shear wave velocities in PSHA results in larger spectral accelerations obtained nonetheless, a median value of the $V_s(30)$

range has been adopted here. Considering the difference between the UHS obtained by a PSHA and the NZS1170 design spectra generally low structural response is expected at given hazard levels where the PSHA spectra are used compared to the response computed based on the NZS1170 spectra.

NZS1170 specifies a design spectrum for 500-year return period hazard intensity. To obtain response spectra at other return periods, as the code stipulates, the spectrum is multiplied by a scale factor (known as *return period factor* in NZS1170) while the shape of the response spectrum is retained. The New Zealand code suggests scaling factors up to 2500-year return period hazard intensity. A linear regression analysis in the logarithmic scale relating the return period to the available code scale factors was carried out to extrapolate the scale factors and to generate design spectra at higher hazard levels.

At each hazard level, GMs are selected, from the Pacific Earthquake Engineering Research (PEER) NGA database such that they best match the site characteristics. Selected GMs fall within a magnitude range of $5 \leq M_w \leq 8$ and source to site distance of $20\text{km} \leq R_{JB} \leq 150\text{km}$. They were produced by strike-slip or reverse faults, and recorded on soils with shear wave velocities within a range of $150\text{m/s} \leq V_s \leq 400\text{m/s}$. Selected ranges of magnitude and distance are based on the two major Canterbury faults and Alpine faults in New Zealand which can produce GMs with different characteristics. Of the GMs with these characteristics, 20 GMs (each with two horizontal components) are selected which, once scaled, best match the target spectrum within a period range of interest (to be explained later). Scaling of the GMs is limited to a factor within a range of $0.4 \leq S_c \leq 2.5$. Although a wide range of magnitude and distance have been chosen to select GMs to include the different source characteristics in the vicinity of Christchurch, the narrow scaling factor limit to match the target spectra is believed to exclude most unrepresentative records.

4.2 *Period range to match selected GMs to a target spectrum*

To match GM records with a target spectrum required for GM selection, several period ranges have been proposed in literature. In this study, the range of period within which the GMs are scaled is decided based on structural characteristics with an intention to rationally account for the effects of higher order modes and softened nonlinear response phase. The lower limit of the period range is computed as the highest modal period whose contribution makes the mass participation exceed 90% of the total mass of the building. This method for determination of the period range implies that for low-rise buildings with regular plans, where most of the modal mass is contributed by the first mode, fundamental period of the structure itself can be used as the lower limit. For the case study building, the effective modal masses for the first and second modes amount respectively to 83% and 9% of the total building mass. Hence, the period of the second mode ($T_2=0.5\text{s}$) is taken as the lower limit of the period range for GM scaling.

The upper limit of the scaling period range is aimed to correspond to the maximum likely post-yielding inelastic response of the structure, and is calculated using the secant stiffness of the structure corresponding to the design ductility as in the following equation:

$$T_e = T_i \left(\frac{\mu}{1+r(\mu-1)} \right)^{0.5} \quad (1)$$

where T_e is the secant period, T_i is the initial period, μ is the ductility factor, and r is the ratio of post-yield to elastic stiffness of the system assuming that the skeleton force-displacement response is represented by a bilinear approximation. Since the r factor is small, Eq. (1) can be simplified to $T_e = T_i(\mu)^{0.5}$. The case study building has been designed for a ductility of 4 ($\mu = 4$) and hence, the upper limit of the period range becomes two times of the initial period, i.e. $T_e = 3.0$

4.3. Selection of ground motions based on CMS and GCIM

The conditional mean spectrum (CMS), as the name implies, provides the mean response spectral ordinates within a period range conditioned on the spectral ordinate at a single period (commonly the natural period of the structure's first mode), and is directly linked to probabilistic seismic hazard analysis (PSHA). Further details on CMS can be available in Baker (2011). To include other characteristics of GMs correlated to the structural response, a generalised conditional intensity measure (GCIM) approach has been recently proposed (Bradley 2010, 2012) in which *IMs* other than S_a can also be used to select GMs. These two methods (i.e. CMS and GCIM) were also used to select and scale (wherever needed) ground motions at different hazard levels to conduct RHAs on the case study building frame in addition to the two UHS based methods described in the previous section.

5 OBSERVATION OF COLLAPSE MECHANISM IN THE ANALYSIS

In order to investigate the simulation of collapse mechanism in the structural model, stress-strain history of a critical section of the case study structure subjected to an example GM record which causes structural collapse is scrutinised. Fig. 4 illustrates the stress-strain history of a section in the column tagged "A" at the elevation view shown in Fig. 2, i.e. the column on the right corner of the frame above the ground level. Fig. 4a shows the stress-strain history of the section for a fiber on the left side of the cross section. Fig. 4b and 4c depict the stress-strain history of two steel fibers on the right and left side of the cross section, respectively. In order to explain the collapse mechanism, the last four stages of the analysis before collapse have been labelled. As can be seen in the figure, failure of the section commences when the strain in the concrete fiber exceeds the crushing strain, i.e. 0.03 in this example (Fig. 4a). By failure of the concrete fiber in compression, the section starts losing capacity to carry compression loads (label 4). In order for the structure to continue sustaining the vertical loads, compression stress is transferred to inner concrete fibers and the steel bars. The column can continue to carry vertical loads (labels 4 to 2) until majority of the concrete fibers lose their compression capacity (label 1) when all the vertical loads are transferred to the steel bars. Eventually,

the section fails due to inability of the reinforcing bars to carry the compression loads. It can be noticed that in the last couple of steps before collapse, both steel fibers are subjected to compressive stress despite being on the opposite sides of the cross section.

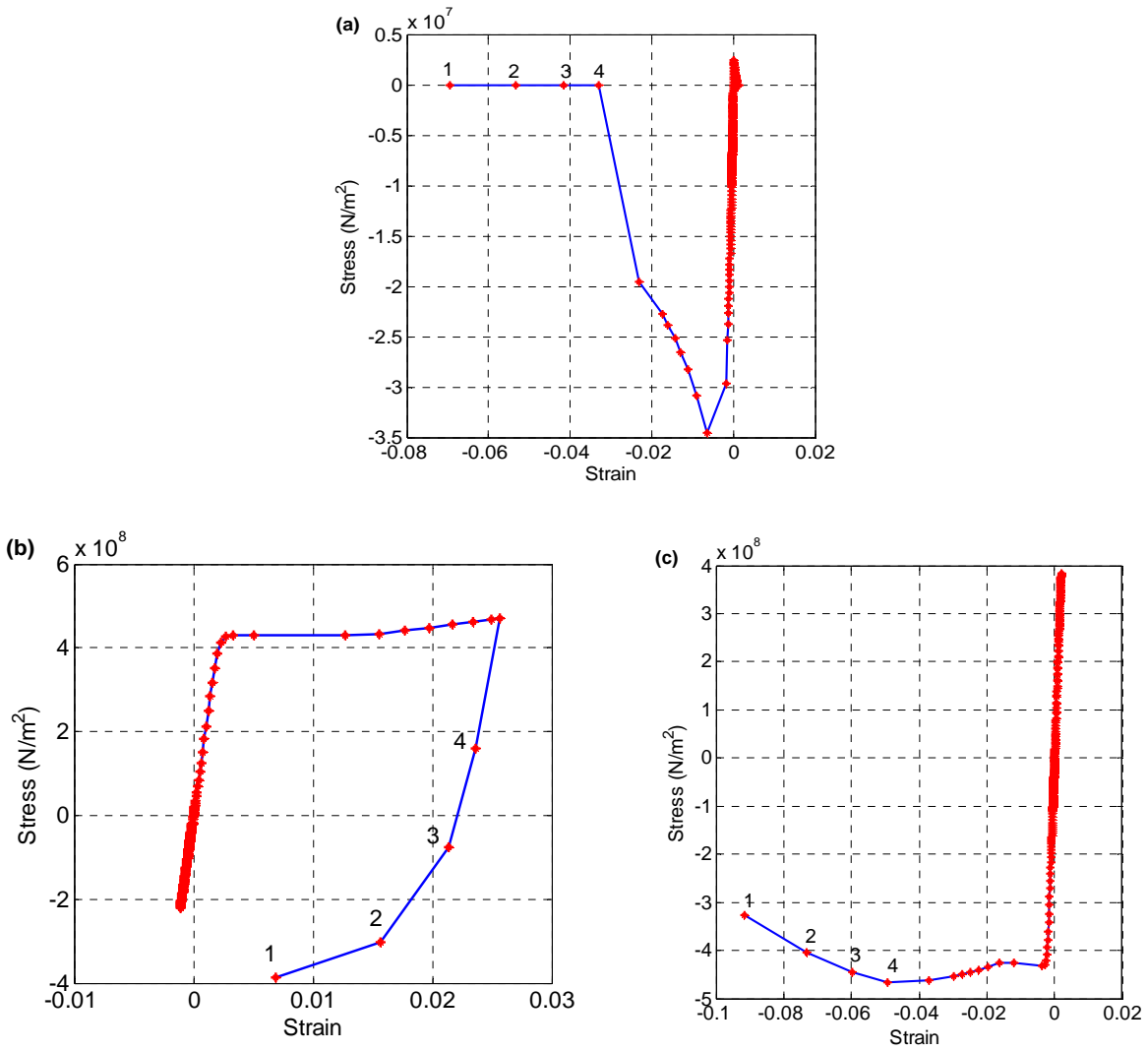


Fig. 4 Stress-strain history of selected fibers of a critical section subjected to an example ground motion (a) A concrete fiber in compression side (b) A reinforcing steel fiber in tension side (c) A reinforcing steel fiber in compression side.

The failure mechanism observed in the structural model implies that collapse of the building occurred in this case due to the loss in vertical load carrying capacity of the structure rather than lack of structural strength to resist destabilizing $P - \Delta$ effects which is the only collapse mode considered by conventional lumped plasticity models. The structural failure starts when the confined concrete strain exceeds the crushing limit which is dependent on confinement configuration of structural components. If a very close confinement is provided in the structural components, particularly at the critical plastic hinge regions, the structure sustains large displacements and collapse may occur due to destabilizing $P - \Delta$ effects.

5 COLLAPSE PROBABILITY OF THE CASE STUDY BUILDING

5.1 Collapse assessment in terms of hazard-based intensity measure

Following the method discussed in section 3, RHAs were performed for 40 selected GMs (two horizontal components of 20 GMs) at hazard levels corresponding to various return periods until the hazard level where more than 50% of the GMs cause collapse. Each component of a GM is applied separately to the structure.

Since GMs are selected based on their probability of exceedance in 50 years, a hazard-based IM such as return period can be used to calculate collapse probability. Fig. 5 illustrates collapse probabilities of the building at various hazard levels acquired by different GM selection approaches. Collapse probabilities are depicted in terms of return period as well as $S_a(T_1 = 1.5s)$. Although the analyses could be stopped for UHS based GMs once the collapse probability exceeded 50%, they were continued for two more hazard levels to achieve more data points to be able to plot the collapse fragility curve with more certainty. It is noted that apart from the NZS1170 method, PSHA was used to estimate the hazard at each intensity level. Consequently, Fig. 5a shows that NZS1170 method results in substantially higher structural responses (and greater collapse probabilities) at a given hazard level compared to other methods. Even among the PSHA based methods, the UHS approach results in a higher response compared to the other two (CMS and GCIM).

5.2 Collapse fragility curves

On the basis of the collapse probabilities of the structure at discrete hazard levels, collapse fragility functions were constructed using various GM selection approaches by fitting the data points to a lognormal distribution. Fragility curves based on four different GM selection methods are shown in Fig. 6. Collapse probabilities at each hazard level can be read from the fragility curves. Table 1 summarizes the results of the collapse performance assessment of the building from the constructed collapse fragility curves.

A close agreement between the fragility curves obtained by two alternatives of UHS in Fig. 6 indicates that although the two variations of UHS differ substantially in terms of interpretation of hazard, they tend to have similar results in terms of spectral acceleration because of the close agreement between the two spectral shapes.

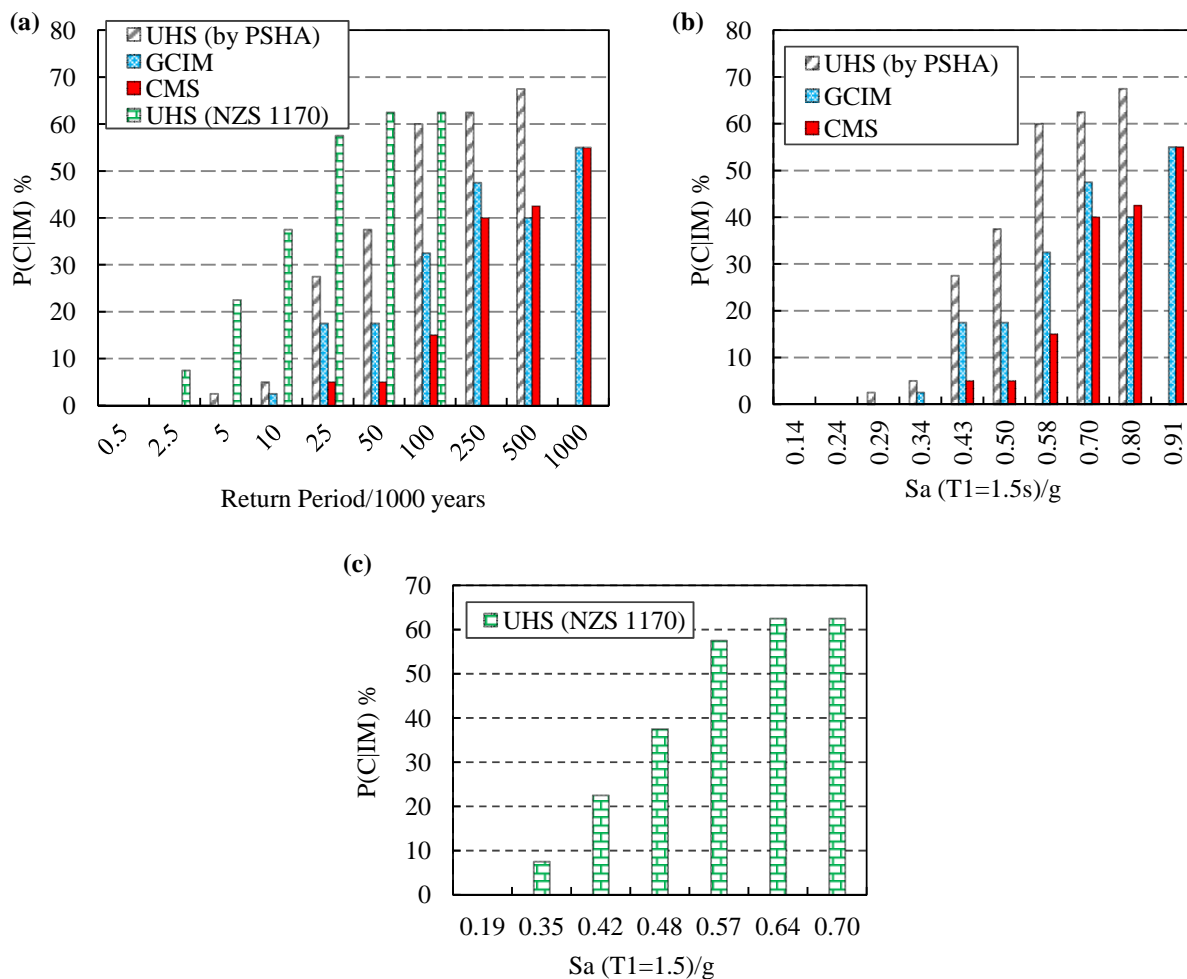


Fig. 5 Collapse probability of the building at various hazard levels assuming cracked period of the structure

IDA-based collapse assessments have reported dispersion in collapse capacity due to record-to-record randomness ranging from 0.35g to 0.45g (Zareian et al. 2010, Liel et al. 2009, Ibarra and Krawinkler 2005, Haselton 2006). Fragiadakis and Vamvatsikos (2010) reported values ranging from 0.30 to 0.4, while FEMA P695 (2009) proposes a value of 0.4. Record-to-record randomness values listed in Table 1 are based on a more rigorous approach of conducting RHAs at discrete hazard levels and based on sophisticated models that are able to capture collapse due to loss of vertical load carrying capacity in addition to P-delta induced lateral destabilisation. Consequently, the uncertainties are larger than the values reported in literature; interestingly despite resulting in more conservative prediction than the other three methods the NZS1170 method resulted in the lowest variability (i.e. less than 0.4 which is comparable to the values reported in literature).

These results suggest that record-to-record randomness in design documents may require revision in future performance-based guidelines.

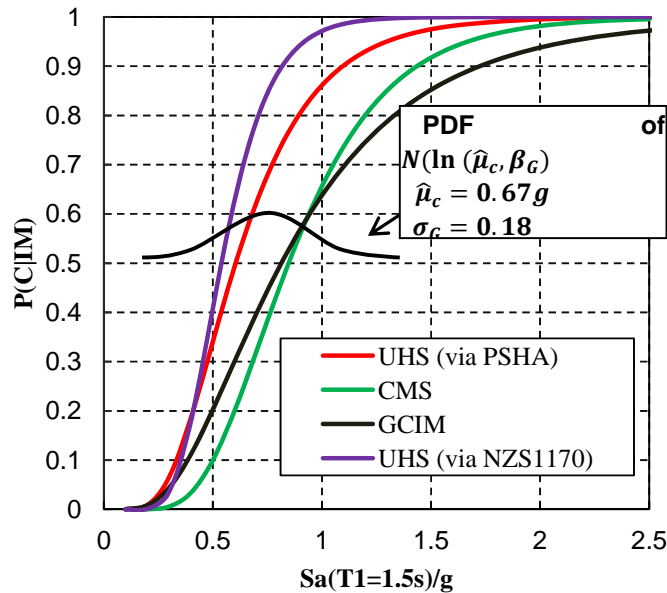


Fig. 6 Collapse fragility curve of the case study building using four different GM selection methods along with the distribution of median collapse capacity assuming cracked period of the structure

Table 1 Results of collapse performance assessment of the case study building assuming cracked stiffness of structural components

GM selection method	Median $S_a(T_1 = 1.5s)$	Record-to-record randomness, β_R	$P(C S_{a_{2/50}} = 0.35g)$
UHS (via PSHA)	0.60g	0.46	12%
UHS (via NZS1170)	0.57g	0.38	11%
CMS	0.85g	0.41	2%
GCIM	0.81g	0.58	8%

6 UNCERTAINTY IN THE ADOPTION OF GM SELECTION METHODS

The collapse probability at given hazard levels can be expressed mathematically as:

$$P(C|S_a) = \Phi\left(\frac{\ln(S_a) - \ln(\mu_c)}{\ln\beta_{TOT}}\right) \quad (5)$$

where $\Phi(*)$ is the standard normal distribution function, and β_{TOT} is the dispersion due to all sources of uncertainties in estimation of the collapse capacity of structures. Sources of uncertainty in quantifying collapse capacity of structural systems are generally differentiated into *aleatory* and *epistemic* uncertainties (Zareian and Krawinkler 2007). The aleatory uncertainty reflects the variability in collapse capacity due to random nature of ground motions (denoted as record-to-record variability). The epistemic uncertainty in literature has generally been introduced due to lack of knowledge about the building's real model. However, results presented in previous sections indicate that adoption of various GM selection methods may lead to different interpretation of performance of the building in terms of collapse capacity. To account for the variability due to GM selection methods a new uncertainty is proposed for consideration in collapse assessment of buildings.

In order to incorporate the effects of GM selection in collapse fragility, β_G can be combined with the epistemic uncertainty and the record-to-record randomness by using the square root of the sum of the squares (SRSS) approach. Hence, the total uncertainty can be computed as:

$$\sigma_{TOT} = \sqrt{\beta_R^2 + \beta_U^2 + \beta_G^2} \quad (6)$$

where β_U is the modelling uncertainty, and β_G is the proposed new source of uncertainty in estimation of collapse capacity using different methods.

Prediction of β_G requires extensive range of analyses with various GM selection methods to observe the variation of median collapse capacity using different methods. For instance, distribution of the median collapse capacities of the case study building due to variability in the GM selection methods is graphically evaluated in Fig. 6. In this case, the median of the median collapse capacity is $\hat{\mu}_c = 0.67g$, which is greater than the median collapse capacity given by the two UHS based methods but less than that from the CMS and GCIM based methods. Similarly, the dispersion in the median collapse capacity; i.e. β_G amounts to 0.18. Inclusion of β_G in collapse estimation facilitates consideration of variability due to different GM selection approaches in performance-based guidelines.

7 SUMMARY AND CONCLUSIONS

A ten-storey RC moment resisting frame building designed based on the NZ standard was used as the case study building to illustrate various aspects of collapse potential of RC buildings. A fiber-element model was introduced which enables accounting for the loss of vertical load carrying capacity in structural model. Observation of the collapse mechanism in the structural model indicates the accuracy of the model in simulation of structural collapse. The fiber model does not require calibration of the model components

in the element level. Degrading behaviour of the structural components is also captured through modelling of buckling and cyclic fatigue deterioration of reinforcing steel.

Despite the use of an improved structural model and methodology for performance assessment of the building in this study, several approximations were made. Apart from the loss of the vertical load carrying capacity and sidesway collapse, other modes of collapse such as shear failure of structural components, punching shear failure in slab-column joints were neglected. Moreover, contribution of slab in structural components stiffness and strength and base flexibility were not accounted for in the structural model.

Instead of using a suite of GMs and uninhibitedly scaling the selected records to represent various hazard intensities, a method was used in which collapse probabilities are estimated by conducting RHAs at discrete hazard levels and fitting them to a lognormal distribution to construct collapse fragility curve. The analyses starts from a hazard level where collapse probability is zero and is continued until more than 50% of the GMs cause collapse. Using RHAs at discrete hazard levels enable definition of hazard-based *IMs* such as return period. Hazard-based *IMs* facilitate comparison of collapse potential of various range of buildings located in the same seismic hazard zone independent of their structural properties. Effect of different GM selection methods was examined on the collapse fragility curve estimation of the case study building. To scale GMs to match with a target spectrum, a period range depending on structural characteristics was proposed.

Collapse probability assessment of the case study building frame indicated a larger record-to-record randomness compared to the values proposed in literature based on IDA results. The GCIM method resulted in the largest variability among the four GM selection methods. Inclusion of the loss of vertical load carrying capacity in the structural model resulted in larger collapse probability in comparison with values reported in literature for ductile structures.

A new source of variability was introduced in the paper to account for the variation due to different GM selection approaches. Availability of different GM selection methods adds a new variability in collapse fragility of buildings. Conventional GM selection based on UHS leads generally to conservative prediction of collapse potential.

REFERENCES

- Baker, J. W. (2011). "Conditional Mean Spectrum: Tool for Ground-Motion Selection." *Journal of Structural Engineering*, 137(3), 0733-9445.
- Baker, J. W., and Allin Cornell, C. (2006). "Spectral shape, epsilon and record selection." *Earthquake Engineering & Structural Dynamics*, 35(9), 1077-1095.
- Bradley, B., and Dhakal, R. P. (2008). "Error estimation of closed-form solution for annual rate of structural collapse." *Earthquake Engineering & Structural Dynamics*, 37(15), 721–1737.
- Bradley, B. A. (2010). "A generalized conditional intensity measure approach and holistic ground-motion selection." *Earthquake Engineering & Structural Dynamics*, 39(12), 1321-1342.

- Bradley, B. A. (2012). "A ground motion selection algorithm based on the generalized conditional intensity measure approach." *Soil Dynamics and Earthquake Engineering*, 40, 48-61.
- Bull, D., and Brunson, D. (1998). "Examples of Concrete Structural Design to New Zealand Standards 3101." New Zealand.
- Chang, G., and Mander, J. (1994). "Seismic Energy Based Fatigue Damage Analysis of Bridge Columns: Part I – Evaluation of Seismic Capacity." *NCEER Technical Report*
- Dhakal, R., and Maekawa, K. (2002a). "Modeling for Postyield Buckled of Reinforcement." *Journal of Structural Engineering*, 128(9), 1139-1147.
- Dhakal, R. P., and Maekawa, K. (2002b). "Path-dependent cyclic stress–strain relationship of reinforcing bar including buckling." *Engineering Structures*, 24(11), 1383–1396.
- Eads, L., Miranda, E., Krawinkler, H., and Lings, D. (2012). "An efficient method for estimating the collapse risk of structures in seismic regions." *Earthquake Engineering & Structural Dynamics*, 42(1), 25-40.
- FEMA (2009). "Quantification of Building Seismic Performance Factors." Federal Emergency Management Agency, Report No. FEMA P695, Washington, DC.
- Fragiadakis, M., and Vamvatsikos, D. (2010). "Fast performance uncertainty estimation via pushover and approximate IDA." *Earthquake Engineering & Structural Dynamics*, 39(6), 683-703.
- Ghafory-Ashtiany, M., Mousavi, M., and Azarbakht, A. (2011). "Strong ground motion record selection for the reliable prediction of the mean seismic collapse capacity of a structure group." *Earthquake Engineering & Structural Dynamics*, 40(6), 691–708.
- Haselton, C. B. (2006). "Assessing seismic collapse safety of modern reinforced concrete moment frame buildings." Ph. D. Thesis, Department of Civil and Environmental Engineering, Stanford University.
- Haselton, C. B., Liel, A. B., Lange, S. T., and Deierlein, G. G. (2008). "Beam-Column Element Model Calibrated for Predicting Flexural Response Leading to Global Collapse of RC Frame Buildings." *Pacific Earthquake Engineering Research Center*, University of California, Berkeley.
- Ibarra, L., and Krawinkler, H. (2005). "Global collapse of frame structures under seismic excitations." *Report No. 152*, The John A. Blume Earthquake Engineering Center, Stanford University, Stanford, CA.
- Ibarra, L. F., Medina, R. A., and Krawinkler, H. (2005). "Hysteretic models that incorporate strength and stiffness deterioration." *Earthquake Engineering & Structural Dynamics*, 34(12), 1489-1511.
- Karthick, M. M., and Mander, J. B. (2011). "Stress-Block Parameters for Unconfined and Confined Concrete Based on a Unified Stress-Strain Model." *Journal of Structural Engineering*, 137(2), 270–273.
- Kunnath, S. K., Heo, Y., and Mohle, J. F. (2009). "Nonlinear Uniaxial Material Model for Reinforcing Steel Bars." *Journal of Structural Engineering*, 135(4), 335–343.
- Liel, A. B. (2008). "Assessing the collapse risk of California's existing reinforced concrete frame structures: Metrics for seismic safety decisions." Stanford University.
- Liel, A. B., Haselton, C. B., and Deierlein, G. G. (2010). "Seismic collapse safety of reinforced concrete buildings. II: Comparative assessment of nonductile and ductile moment frames." *Journal of Structural Engineering*, 137(4), 492-502.
- Liel, A. B., Haselton, C. B., Deierlein, G. G., and Baker, J. W. (2009). "Incorporating modeling uncertainties in the assessment of seismic collapse risk of buildings." *Structural Safety*, 31(2), 197-211.

- Lignos, D. G., and Krawinkler, H. (2010). "Deterioration modeling of steel components in support of collapse prediction of steel moment frames under earthquake loading." *Journal of Structural Engineering*, 137(11), 1291-1302.
- Lignos, D. G., and Krawinkler, H. (2012). "Development and utilization of structural component databases for performance-based earthquake engineering." *Journal of Structural Engineering*.
- Mander, J. B., Priestley, M. J. N., and Park, R. (1988). "Theoretical Stress-Strain Model for Confined Concrete." *Journal of Structural Engineering*, 114(8), 1804–1826.
- NZS1170.5 (2004). "Structural Design Actions part 5: Earthquake Actions New Zealand." *Standards New Zealand* Wellington, New Zealand.
- OpenSees (2012). "Open System for Earthquake Engineering Simulation ", Pacific Earthquake Engineering Research Centre, University of California, Berkeley.
- Popovics, S. (1973). "A numerical approach to the complete stress strain curve for concrete." *Cement and concrete research*, 3(5), 583-599.
- Vamvatsikos, D., and Cornell, A. (2002). "Incremental Dynamic Analysis." *Earthquake Engineering & Structural Dynamics*, 31, 491-514.
- Zareian, F., and Krawinkler, H. (2007). "Assessment of probability of collapse and design for collapse safety." *Earthquake Engineering & Structural Dynamics*, 36, 1901-1914.
- Zareian, F., Krawinkler, H., Ibarra, L., and Lignos, D. (2010). "Basic concepts and performance measures in prediction of collapse of buildings under earthquake ground motions." *Structural Design of Tall and Special Buildings*, 19, 167-181.